

# Measurement of the spatial degree of coherence in a Lloyd's Mirror interferometer



**Celso L. Ladera, Guillermo Donoso and E. Stella**

*Departamento de Física, Universidad Simón Bolívar, Valle de Sartenejas,  
Caracas 1089, Edo. Miranda, Venezuela.*

**E-mail:** clladera@usb.ve

(Received 3 October 2017, accepted 15 December 2017)

## Abstract

We present a low-cost experiment, suitable for undergraduate teaching laboratories, in which the concept of degree of coherence is introduced. The spatial degree of coherence of a Lloyd's Mirror wavefront-division interferometer has been measured as a function of the separation between its point-like real source and the virtual image of the source given by the mirror. The mirror was irradiated with temporally coherent divergent spherical waves from a pinhole illuminated with He-Ne laser light. Given the close similarity between the Young and Lloyd interferometers similar spatial degrees of coherence dependences were expected, yet it was found that this is not the case: the degree of coherence in the later case was found to be nearly quadratic with respect to the distance between the two light sources of the Lloyd interferometer.

**Keywords** Lloyd's mirror interferometer, spatial degree of coherence, two-beam interferometry.

## Resumen

Presentamos un experimento de bajo costo, adecuado para los laboratorios de enseñanza de pregrado, en el que se introduce el concepto de grado de coherencia. El grado espacial de coherencia de un interferómetro de división de onda del espejo de Lloyd se ha medido como una función de la separación entre su fuente real puntual y la imagen virtual de la fuente dada por el espejo. El espejo fue irradiado con ondas esféricas divergentes temporalmente coherentes desde un agujero iluminado con luz láser He-Ne. Dada la estrecha similitud entre los interferómetros Young y Lloyd, se esperaban grados espaciales similares de dependencias de coherencia, pero se encontró que este no es el caso: el grado de coherencia en el último caso resultó ser casi cuadrático con respecto a la distancia entre las dos fuentes de luz del interferómetro Lloyd.

**Palabras clave:** Interferómetro de espejo de Lloyd, grado espacial de coherencia, interferometría de dos haces.

**PACS:** 42.25Kb, 42.25Hz

**ISSN 1870-9095**

## I. INTRODUCTION

The classic and well-known two-beam Mirror interferometer of H. Lloyd, that dates from 1834, is presently and somehow surprisingly being used – because of its simplicity and compactness– in at least three recent and important technological applications: in extreme UV photolithography of wafers [1]; in the so-called nanopatterning techniques [2], and in writing Bragg gratings in optical fibres [3]. The setup of the Lloyd interferometer is simple, very easy to assemble, and indeed of very low-cost [4]. It is easier to set up than the better known two-beam Young interferometer. It thus represents an interesting and efficient alternative for studying the interference of light in introductory physics laboratories or showing it in lecture demonstrations. One interesting issue is the observation of the black first order fringe in Lloyd interference patterns that is to be compared with the first order bright fringe observed

in Young interference patterns. In this work we present a more advanced issue: the results of our measurements of the spatial degree of coherence of a Lloyd interferometer, the interferometric figure of merit which is known to be of great interest for applications of interferometers e.g. the spatial degree of coherence is very relevant for the recent cases of synchrotron radiation and X-ray interference measurements with a Young's interferometer [5] whose geometry is shown in Fig. 1, and as already said very similar to the Lloyd's Mirror interferometer geometry shown in Fig. 2.

Because of its importance in optics the spatial degree of coherence of an extended optical source has already been measured using for instance speckle interferometry [6, and references there in]. Let us here begin with a brief introduction to the key concepts of the important theory of Coherence, this time in relation to Interference [7].

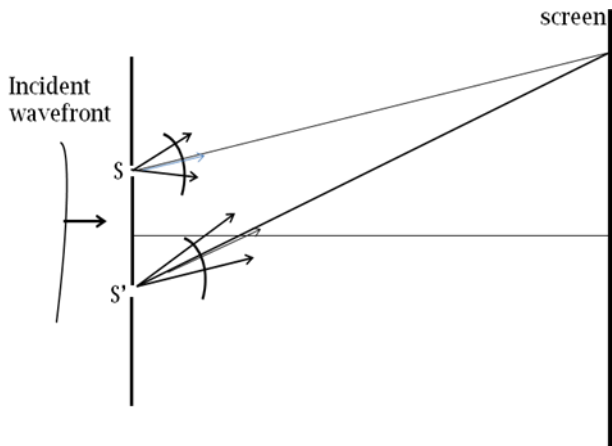


**FIGURE 1.** Scheme of a Young interferometer set-up: S and S' are two real point-like or narrow slits sources of light that actually sample the incident wavefront at two different points ( $\mathbf{r}_1, \mathbf{r}_2$ ).

Given a light wavefront its *spatial degree of coherence* is defined as a statistical correlation between the complex stationary electric field amplitudes  $A(\mathbf{r}_1, t)$  and  $A(\mathbf{r}_2, t)$  of the wavefront two different points ( $\mathbf{r}_1, \mathbf{r}_2$ ) and at the same given time  $t$ . The *temporal degree of coherence* instead is a statistical correlation between the stationary complex amplitudes at two different times ( $t, t + \tau$ ), along a given field wavetrain, for a given delay  $\tau$ . The theoretical and scalar *mutual degree of coherence*  $\Gamma$  is then defined as the correlation function that represents both the spatial and the temporal coherence, and it is given by the second order average,

$$\Gamma(\mathbf{r}_1, \mathbf{r}_2; \tau) = \langle A(\mathbf{r}_1, t)A^*(\mathbf{r}_2, t + \tau) \rangle_t$$

$$= \lim_{T \rightarrow \infty} \frac{1}{2T} \int_{-T}^T A(\mathbf{r}_1, t)A^*(\mathbf{r}_2, t + \tau) dt, \quad (1)$$

For the case of the well-known Young' interferometer, and in general for any two-beam interferometers, the *normalized complex degree of coherence*  $\gamma_{12}$  is given by

$$\gamma_{12} = \gamma(\mathbf{r}_1, \mathbf{r}_2; \tau) = \frac{\Gamma(\mathbf{r}_1, \mathbf{r}_2; \tau)}{\sqrt{I_1 I_2}}, \quad (2)$$

where  $I_1$  and  $I_2$  are the irradiances (or intensities) of the two interfering beams at the plane where the interferograms are observed. The irradiance  $I(\mathbf{r})$  at a given point  $\mathbf{r}$  of the interference pattern is given by the well-known relation

$$I(\mathbf{r}) = I_1 + I_2 + 2\gamma_{12}(\tau)\sqrt{I_1 I_2} \cos \varphi_{12}(\mathbf{r}), \quad (3)$$

where  $\varphi_{12}(\mathbf{r})$  represents the phase difference at that point. The so-called *contrast* or *visibility*  $V$  of interference patterns may be defined as

$$V = \frac{I_{max} - I_{min}}{I_{max} + I_{min}}, \quad (4)$$

where  $I_{max}$  and  $I_{min}$  are the maximum and minimum field irradiances observed in the interference pattern. When expressions for these two irradiances are obtained from Eq. (3) and replaced into Eq. (4) the following expression for the degree of coherence  $\gamma_{12}$  ensues,

$$\gamma_{12} = \frac{V(I_1 + I_2)}{2\sqrt{I_1 I_2}}. \quad (5)$$

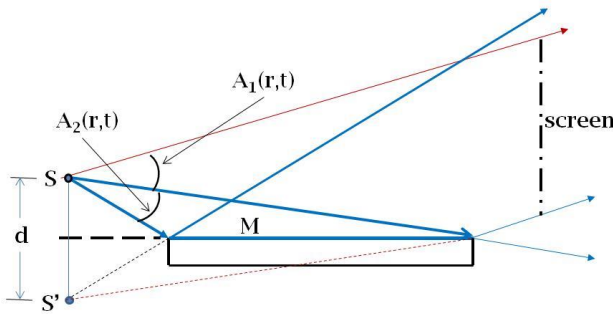
It may be seen that for equal beam irradiances  $I_1 = I_2$  the degree of coherence becomes equal to the contrast  $V$ . As it shall be seen such equality between those two irradiances never occurs for the case of the Lloyd mirror interferometer (see Figs. 2 and 9). It may also be seen all quantities in Eq. (5) are experimentally measurable and thus such expression is the one usually used for measuring the spatial degree of coherence for any two-beam interferometer in the laboratory. It is known that both the visibility and the spatial degree of coherence of the Young's interferometer depend upon the local optical path variations that may arise in the region between the two sources  $\mathbf{S}$  and  $\mathbf{S}'$  of coherent light and the screen of observation (e.g. because of changes in the refractive index of an optical medium that may exist between sources and the screen of observation) as well as upon the pertinent separation  $d$  between the two sources of the beams. This was already shown by Thompson and Wolf [8] for the case of the Young's interferometer.

We have thus measured the spatial degree of coherence  $\gamma$ , as given by Eq. 5, of our Lloyd's wavefront-division interferometer as a function of the very pertinent separation  $d$  between its real point-like source  $\mathbf{S}$  – actually a pinhole irradiated with temporally coherent converging spherical waves – and the virtual image  $\mathbf{S}'$  of such source in the flat mirror, both shown in Fig. 2. Our experimental results show that the measured spatial coherence  $\gamma$  of the Lloyd's interferometer is a quadratic function of that separation  $d$ . Such dependence was obtained by replacing both (i) the measured visibility values of the observed interferograms and (ii) the measured separate functional dependences of the integrated irradiances  $I_1$  and  $I_2$  of the two interfering beams, i.e. the irradiance of the direct beam from the point-like source and the irradiance of the beam reflected from the mirror – into the theoretical expression of the spatial coherence ( $\gamma$ ). The two irradiances were independently measured as functions of the separation  $d$  between the two point sources. The experiments and measurements presented in this work are really low-cost and thus very suitable for intermediate and advanced physics laboratory courses taken by physics majors.

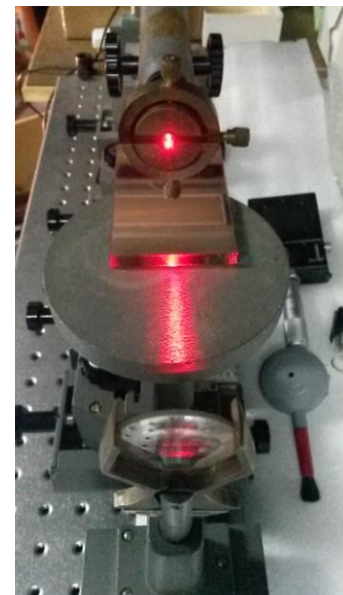
## II. EXPERIMENTAL SET-UP

Figure 2 shows a geometrical scheme of our Lloyd's interferometer setup. The real point-like source  $\mathbf{S}$  is a 15  $\mu\text{m}$  diameter spatial filtering pinhole irradiated with coherent converging spherical waves from a well-corrected 20X achromatic microscope objective of numerical aperture 0.40,

and 9 mm focal length. A collimated unpolarized TEM-00 beam (0.81 mm diameter at  $1/e^2$  of maximum irradiance) from a 5 mW He-Ne laser (not shown in the scheme) was sent into the microscope objective that focused the beam into the pinhole. The pinhole thus performed as a filter in the standard and well-known spatial filtering configuration. A diverging spherical electric field wavefront, of Gaussian profile, emerges from such pinhole, a portion  $A_1(\mathbf{r},t)$  of which travels to the right while another portion  $A_2(\mathbf{r},t)$  is reflected by the mirror (shown in Figs. 2 and 3). The 75 mm long and 45 mm wide flat metallic mirror M has a reflectance of about 95 %. It was seated on a flat horizontal circular table fixed to a kinematic mount resting on a heavy optical bench. The pinhole was placed about one centimetre above the level of the mirror. The kinematic mount allowed us to vertically move the table and mirror smoothly, and with about 0.1 mm resolution. The interferograms between the two beams were observed on a screen placed far away, actually at about 2.40 m to the right of the mirror (Fig. 2). The actual experimental setup is presented in figure 3, and a picture of it is portrayed in Fig. 4.



**FIGURE 2.** Geometry of Lloyd's interferometer. **S** is a real light point source at distance  $d$  from its virtual image **S'** on the flat mirror **M**.  $A_1(\mathbf{r}, t)$  and  $A_2(\mathbf{r},t)$  denote the electric field amplitudes of two portions of a diverging spherical wavefront from **S**. After reflection at the mirror **M** the wavefront  $A_2(\mathbf{r},t)$  travels to the right and superpose with the expanded direct wavefront  $A_1(\mathbf{r},t)$  to produce an interference pattern on a far screen.



**FIGURE 4.** Picture of the Lloyd experimental setup showing the laser at the top and the converging lens at the bottom; the bright irradiating pinhole is clearly seen.

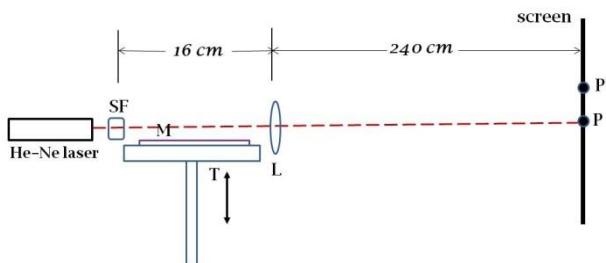


**FIGURE 3.** Lloyd mirror interferometer setup. SF is the spatial filtering system placed above the plane of a flat metallic mirror **M**. The table **T** can be smoothly translated up and down. **L** is a converging lens. **P** and **P'** are images of points **S** and **S'** (see Fig 2). When the lens **L** is removed one can observe the interferograms on the screen.

The irradiances or intensities  $I_1$  and  $I_2$  of the two interfering beams were measured with a highly-linear and small sensitive area PIN photodiode (Hamamatsu S-1087) at the two point images **P** and **P'**, just before one removes the lens to observe the expected interferograms. A small linear array of 250 photodiodes was used to measure the separation  $s'=PP'$  when the two point images **P** and **P'** were too close to be discerned with the photodiode. Neutral density filters were used when necessary to attenuate the light beams thus avoiding the saturation of the photo detectors used in the experiments. As explained below the Lloyd interferograms are only observed when the distance  $PP'=d'$  between the point images is reduced to less than 1cm.

### III EXPERIMENTS AND ANALYSIS OF THE INTERFEROGRAMS

Once the Lloyd mirror is irradiated with the spatially filtered laser beam, and with the converging lens placed in the set-up (Fig. 3 and 4), one may observe the two image points **P** and **P'** on the flat screen placed at 240 cm. If the distance  $PP'=d'$  is a few centimetres and with the converging lens removed what one observes in the screen, most of the times, are two similar and separated diffraction patterns (not the expected Lloyd's interferogram pattern). These two diffraction patterns arise from diffraction at the two straight edges of the mirror, the upper diffraction pattern corresponding to the mirror straight edge closer to the illuminating pinhole (Fig. 2). To observe the expected Lloyd interferograms one has to move the mirror upward, by raising the table T (Fig. 3) that supports it, until the two diffraction patterns gradually overlap, it is only then that one can observe on the screen the expected interference pattern of equally separated fringes.

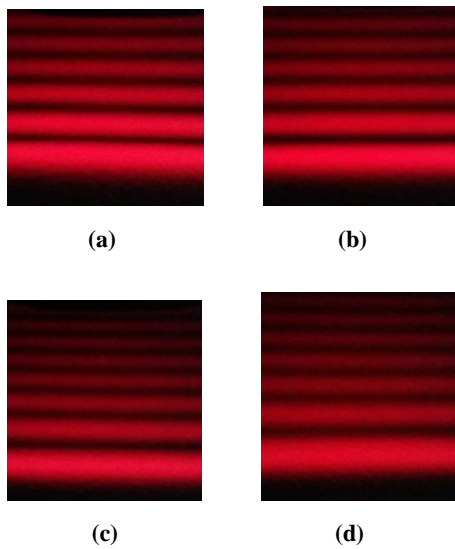


**FIGURE 5.** Observed interference patterns on a screen placed 240 cm to the right of the converging lens L of Fig. 3 for four different values of the sources separation  $d = SS'$ : (a)  $d = 0.33 \text{ mm}$ , (b)  $d = 0.30 \text{ mm}$ , (c)  $d = 0.27 \text{ mm}$ , (d)  $d = 0.23 \text{ mm}$ . Note the first zeroth-order black fringes and the visibility deterioration if the interferograms as  $d$  varies.

Images of the interferograms observed on the flat screen placed at 240 cm from the lens were captured with a CCD camera and then processed with an image processor (Java based *Image-J* processor [9]). Figure 5 shows a sample of four interferograms for four different values of the small separation  $d = SS'$  between the sources of the interfering beams. This small separation is actually obtained by simply measuring the larger separation  $d'$  of the two images **P** and **P'** on the observation screen (see Fig. 3) and then calculating the two sources separation  $d$  using the basic geometrical optics relation between the magnification  $M$  of a lens and the sizes of a given object and its geometrical image (in the

present case  $M=15$ ). Thus a separation  $PP'= 5 \text{ mm}$  corresponds to the two sources separation  $d= SS'=5 \text{ mm}/15=0.33 \text{ mm}$ . Note that the first fringe in all the interferograms is a black one. This is as expected since the lower beam (Fig. 2) undergoes a  $180^\circ$  phase shift upon reflection at the metallic mirror. Figure 6 shows two of the resulting irradiance profile plots that correspond to two of the interferograms shown in Fig. 4 (a), (b) for distances  $d=0.33 \text{ mm}$ , and  $d=0.23 \text{ mm}$  respectively.

The irradiance plots in Fig. 6 are directly given by the image processor facilities called “Line” and “Plot profile” used to process the interferograms images. These facilities allows the image processor to imitate a *microdensitometer* i.e. to scan the interferograms along a straight line in any arbitrary direction chosen by the user, and then giving the optical density along it; in our case the interferograms were scanned in the orthogonal direction to the interference fringes. The differences in contrast of the interferograms irradiance plots in Fig. 4 are clearly appreciable, showing the variation of the spatial degree of coherence with distance  $d$ .

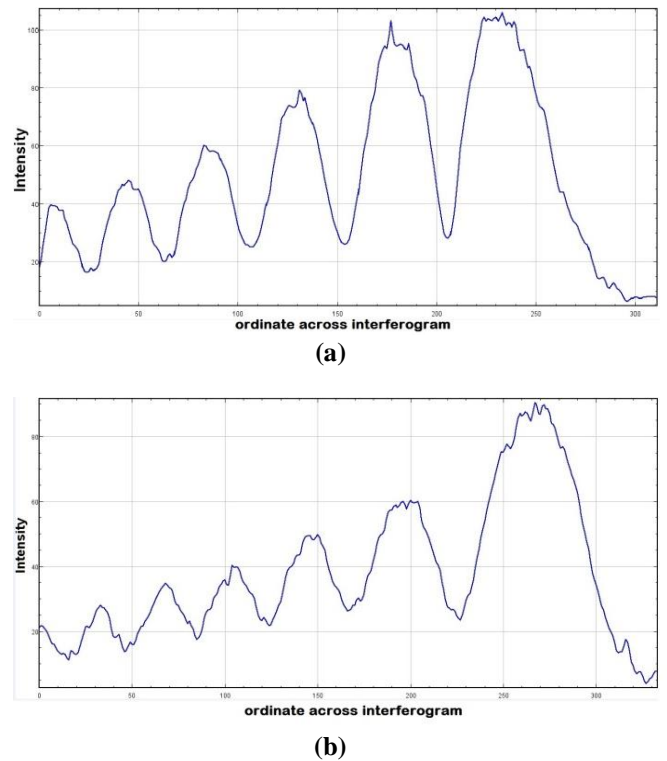


**FIGURE 6.** Intensity or irradiance (in arbitrary units) of two interferograms vs an ordinate across the fringes, plotted for two values of the distance  $d = SS' = 0.33 \text{ mm}$  and  $0.23 \text{ mm}$ .

In figure 7 we have plotted the measured values of the visibilities of the observed interferograms against the two sources separation  $d$ . A non linear, actually nearly quadratic, dependence of the visibility is observed. A maximum is

reached at about  $d=0.27\text{ cm}$ , and the visibility decays monotonically at both sides of the maximum.

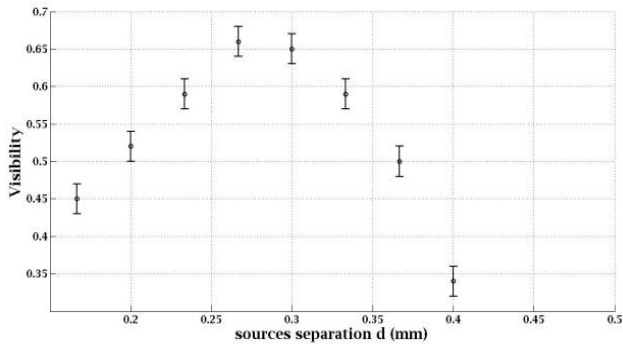


**FIGURE 7.** Plot of the measured visibilities of the interferograms: Visibility versus the sources separation  $d=SS'$

**A. Evaluation of the degree of coherence**

Sets of eight different interferograms images were obtained by varying the vertical position of the horizontal mirror with respect to the pinhole, each set for eight increasing distances  $d$ . Their images were then image-processed and the resulting sets of visibilities obtained. Pairs of corresponding irradiances  $I_1$  and  $I_2$  were also measured with a PIN photodiode as already explained in Section II. The degree of spatial coherence was then calculated by replacing the set of measured visibilities and the set of measured irradiances into Eq. (5). Figure 7 show the plot obtained for the eight values of the sources separation  $d$ . Simple observation of the plotted data suggests that the spatial degree of coherence of the Lloyd Interferometer follows a quadratic behaviour. We have thus calculated and plotted in Fig. 6 a quadratic polynomial fitting curve given by  $D(d)=-0.07971+10.5896d-192504d^2$ , that closely fits the experimental data.

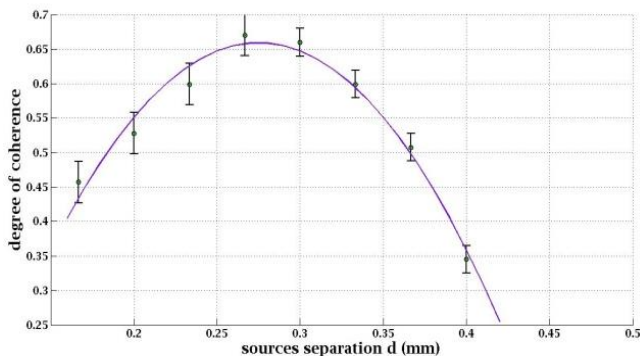


**FIGURE 8.** Plot of the degree of coherence  $\gamma$  data (in circles) as a function of the sources distance  $d$ . The continuous curve is the quadratic polynomial fitting given by  $D(d)=-0.07971+10.5896d-192504d^2$  where  $d$  is measured in cm.

**B. Irradiances of the two interfering beams as a function of the distance  $d'=PP'$**

In search for an experimental justification for the quadratic dependence of the spatial degree of coherence upon the distance  $d'=SS'$ , obtained in Fig. 7 we undertook the task of measuring the dependence of each of the two interfering beam irradiances  $I_1$  and  $I_2$  with respect to the separation  $PP'$  between the two images  $P$  and  $P'$  which was varied, once again by adjusting the position of the flat mirror with respect to the illuminating pinhole. The separate plots of both  $I_1$  and  $I_2$  versus the sources distance  $d$  are shown in figure 8, and correspond to the case when the horizontal distance from the pinhole  $S$  to the left (closer) edge of the mirror was 0.3 cm. Quite unexpectedly both set of data points seem to show that the two irradiances  $I_1$  and  $I_2$  are separately increasing exponentials with respect to the independent variable  $d$ .

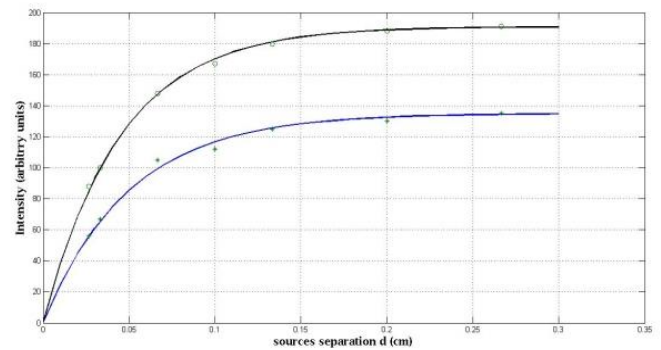


**FIGURE 9.** Plots of the separate irradiances  $I_1$  (circles) and  $I_2$  (asterisks) versus the sources separation  $d$ , when the horizontal distance from the pinhole to the left edge of the mirror was 0.3 cm. Continuous curves are increasing exponential fittings:  $I_1=191[1-\exp(-d/0.045)]$  for  $I_1$ , and  $I_2=135[1-\exp(-d/0.050)]$  for  $I_2$ .

We then fitted the two irradiance data plots with the two increasing exponential curves shown in Fig. 9: fitting curve  $I_1=191 [1-\exp(-d/0.045)]$  for irradiance  $I_1$ , and  $I_2=135 [1-\exp(-d/0.05)]$  for irradiance  $I_2$ . To ensure that the two exponential dependences of the beam intensities  $I_1$  and  $I_2$  were not a matter of chance we repeated the measurement varying the horizontal distance from the pinhole to the left edge of the mirror and the results are presented in the Appendix. This time we set such distance to 4 cm which resulted in interferograms of poorer visibilities (when compared with ones obtained when such distance was 0.3 cm).

Also note that the non-linear behaviour of the visibility curve shown in Fig. 7 dominates the exponentially increasing behaviour of the intensities shown in Fig. 9) resulting in the nearly quadratic behaviour of the degree of coherence when the distance  $d'=PP'$  is diminished to less than about 8 mm (corresponding to  $d$  being about 0.5 cm). It should be noted from Fig. 9 that in the small domain (0.04, 0.02) both intensities  $I_1$  and  $I_2$  do not vary too much, and thus the nonlinear behaviour of the visibility dominates (this can be

readily checked using the equations given in the legend of Fig. 9).

#### IV. CONCLUSIONS AND DISCUSSION

We have measured the spatial degree of coherence of a Lloyd mirror interferometer and obtained a near quadratic dependence of such degree with respect to the two point-like sources of the interferometer. This dependence drastically differs from the well-known profile of the measured spatial degree of coherence in the case of the Young interferometer initially obtained decades ago by Thompson and Wolf [7]. Ours is a low cost experiment, suitable for the intermediate and advanced physics teaching laboratories, and an ideal experiment to introduce the sophisticated concept of degree of coherence to undergraduate students. This work can be extended to obtain an analytic expression for the degree of coherence of the Lloyd interferometer, and verify it in the laboratory.

#### ACKNOWLEDGEMENTS

We acknowledge engineers Guillermo Villegas and Eva Mora (Physics Laboratories and Electronics Laboratories, of Universidad Simón Bolívar, respectively) for their assistance with software and hardware, and the partial support of our Decanato de Investigaciones y Desarrollo under grant GID-073

#### APPENDIX

We repeated the measurement of the two beam intensities to check that the results already obtained in Fig. 9 could be consistently obtained. To the effect we increased the distance from the left edge of the mirror (Fig. 3) to the irradiating pinhole to about 4 cm and again measured both intensities as the distance  $D'$  was decreased. The results appear plotted below, in Fig. A-1.

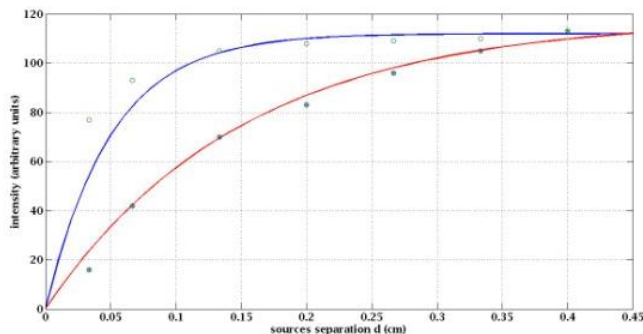


**FIGURE A-1.** Plots of the separate irradiances  $I_1$  (circles) and  $I_2$  (asterisks) versus the sources separation  $d$ , when the horizontal distance from the pinhole to the left edge of the mirror was 4 cm. Continuous curves are increasing exponential fittings:  $I_1=112 [1-\exp(-20d)]$  for irradiance  $I_1$ , and  $I_2=112 [1-\exp(-6,67d)]$  for irradiance  $I_2$

We fitted the two irradiance data plots with the two increasing exponential curves shown in Fig. A-1: fitting curve  $I_1=112 [1-\exp(-20d)]$  for irradiance  $I_1$ , and  $I_2=112 [1-\exp(-6,67d)]$  for irradiance  $I_2$ . It may be seen that the two intensities  $I_1$  and  $I_2$  again show increasing exponential dependences with the separation  $d$  between the two sources  $S$  and  $S'$ , as was found for the case when the distance from pinhole to the left edge of the mirror was 0.3 cm. This finding has been confirmed in not less than eight runs of the experiment.

#### REFERENCES

- [1] Solak, H. H., He D, Li W., Singh-Gasson, S., Cerrina, F., Sohn B. H., Yang X. M. and Nealey, P., *Exposure of 38 nm period grating patterns with extreme ultraviolet interferometric lithography*, *App. Phys. Lett.* **75**, 2328-2330 (1999).
- [2] Wachulak, P. W, Capeluto, M. G, Menoni C. S., Rocca, J. J. and Marconi, M. C., *Nanopatterning technique in a compact setup using table top extreme ultraviolet lasers*, *Opto-electronics Review* **16**, 444–450 (2008).
- [3] Martinez, C and Ferdinand, P., *Phase shifted Bragg grating using a phase plate in a modified Lloyd mirror configuration*, *Electron. Lett.*, **34**, 1687-1688 (1995).
- [4] Kallard, T. *Exploring Laser Light*, Opto-sonic, (Press New York, 1977).
- [5] Lin, J. J., *Measurement of the Spatial Coherence Function of Undulator Radiation using a Phase Mask*, *Phys. Rev. Lett.* **90**, 074001 (2007).
- [6] Ladera, C. L. and Bautista, M, *Measuring the sopatial coherence of a quasi-monochromatic light source using double-exposure speckle interferometry*, *Opt. Letters* **17**, 825-827 (1992).
- [7] Mandel, L. and Wolf, E., *Optical Coherence and Quantum Optics* Ch. 4, (Cambridge Univ. Press., Cambridge, 1995).
- [8] Thompson, B. J. and Wolf, E., *Two-beam interference with partially coherent light*, *J. Opt. Soc. Am.* **47**, 895-902 (1957).
- [9] Schneider, C. A., Rasband W. S. and Eliceirim K. W., *Nature methods* **9** (7): 671-675 (2012). Image-J is a Java based free-download image processor from the N.I.H. of the USA.